A New Fin-Line Ferrite Isolator for Integrated Millimeter-Wave Circuits

ADALBERT BEYER AND KLAUS SOLBACH, MEMBER, IEEE

Abstract—A ferrite isolator in fin-line technique is investigated both theoretically and experimentally. Since fin-line field distributions exhibit similar properties, the realization of a field displacement isolator is possible applying the principles of operation known from metal waveguide isolators. A field expansion method for a simplified isolator model is presented for the investigation of the field theoretical problem. Furthermore the feasibility of the fin-line field displacement approach for the realization of an isolator is demonstrated experimentally at the model frequency of 11 GHz.

I. Introduction

In recent years fin lines have emerged as a useful medium for integrated millimeter-wave circuits. Filters and couplers [1], detector and mixer circuits [2], and even semiconductor oscillator configurations [3] successfully have been realized in the frequency range of 8–170 GHz using fin lines. Although nonreciprocal circuit elements like circulators and isolators are highly useful building blocks in millimeter-wave subsystems, so far no efforts have been made to realize such circuits in fin-line technique. This contribution describes the concept and a first experimental realization of a fin line ferrite isolator at a model frequency (11 GHz).

II. The Concept

Several studies of fin-line dispersion and characteristic impedance have been published [4]–[6], but no field distributions have been given up to now. Since a concept for a ferrite isolator would have to be based on an understanding of the fields of fin line, field distributions have been calculated using the field-theoretical method described in [6].

In Fig. 1 the cross-sectional view of a unilateral fin line is shown together with the E_y-, E_x-, and H_z-field strengths calculated in plane $y=0$ at 11 GHz. The fin-line structure employed here had a slot width of $2s=3.0$ mm, substrate thickness $w=0.25$ mm, $\epsilon_r=10.5$ with a characteristic impedance of $Z_0=185\ \Omega$. The fin-line mount used here was a standard X-band waveguide.

Manuscript received April 13, 1981; revised July 29, 1981.

A. Beyer is with the Fachgebiet Allgemeine und Theoretische Elektrotechnik, FB 9, Department of Electrical Engineering, Duisburg University, Bismarckstrasse 81, D-4100 Duisburg 1, Federal Republic of Germany.

K. Solbach was with the Department of Electrical Engineering, Duisburg University, Duisburg, Federal Republic of Germany. He is now with AEG-Telefunken, Geschaeftsbereich Hochfrequenztechnik, A1E 32, D-7900 Ulm, Federal Republic of Germany.

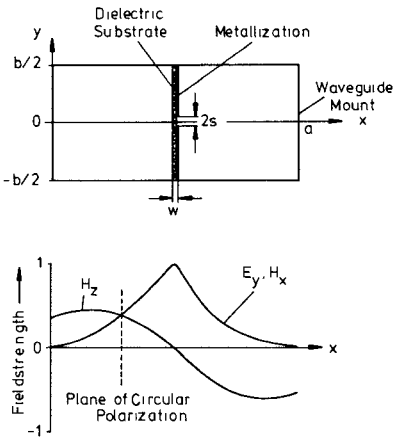

Fig. 1. Fin-line structure with calculated E_y-, H_x-, and H_z-field strengths (X-band mount with $a=22.86$ mm and $b=10.16$ mm).

From the field distributions it can be seen that the propagating wave is concentrated in the neighborhood of the slot. Circularly polarized magnetic fields ($|H_x|=|H_z|$) exist in a plane closer to the center of the waveguide than in unloaded metal waveguide.

It is known that a magnetized ferrite slab placed in a plane of circularly polarized magnetic field exhibits different phase shifts and attenuations for both directions of the propagating waves. Resonance isolators exploiting this phenomenon employ very thin slabs of ferrite to make use of the marked resonance characteristic of the ferrite effective permeability for one direction of propagation.

Field displacement isolators on the other hand employ thick ferrite slabs. The position of the slab has to be chosen so that a condition exists where the field distributions differ very much for both directions of propagation. Under such a condition, appropriately positioned absorbing material inside the waveguide will discriminate between the directions of propagation and thus attenuate waves in one direction (isolation), while the waves in the opposite direction (transmission) are hardly affected [7], [10].

Since the field displacement isolator principle is known to be more effective and broad band as compared to the resonance isolator principle it was decided to make use of it in the design of a fin-line device. The application of the principles of operation known from metal waveguide isolator structures is straightforward since from Fig. 1 it is clear that similar conditions concerning the magnetic field exist in the fin-line structure.

0018-9480/81/1200-1344$00.75 ©1981 IEEE

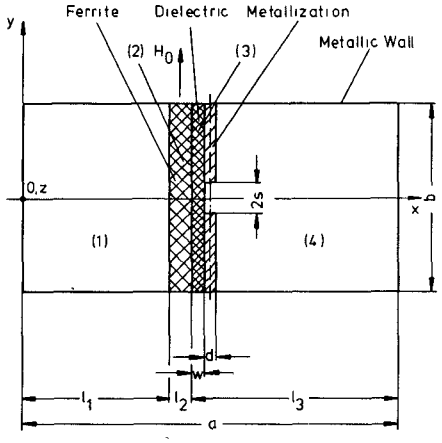

Fig. 2. Cross-sectional structure used in the theoretical investigation of the fin-line isolator.

III. Theoretical Investigation

For a theoretical investigation of the fields in a ferrite-loaded fin line a simple cross-sectional structure was chosen as a model (Fig. 2).

The field-expansion method [6] for the calculation of the field distributions and the phase constants of the fin line can be applied to the cross-sectional structure shown in Fig. 2, if in the additional ferrite slab the fields are expanded in terms of trigonometric functions and the continuity conditions at the ferrite boundaries are incorporated into the original set of equations for the fin-line problem.

In the investigations it was assumed that the fin line as well as the ferrite slab are lossless and the fin-line metallization is infinitely thin ($d \cong 0$).

With respect to the symmetry of the cross-sectional structure only TE-modes are assumed in the expansion of the fields. The time dependence of the waves is assumed to be described by $\exp[j(\omega t - \beta z)]$, where ω is the angular frequency and β is the phase constant of the guided waves.

The magnetic potential functions chosen in the four subregions were

$$\Psi^{(1)} = \sum_{n=0}^{\infty} A_n \cos\left(k_{xn}^{(1)} x\right) \cos\left[\frac{n\pi}{b}(y - b/2)\right], \qquad 0 \leq x \leq l_1 \quad (1)$$

$$\Psi^{(2)} = \sum_{n=0}^{\infty} B_n \sin\left(k_{xn}^{(2)} x\right) \cos\left[\frac{n\pi}{b}(y - b/2)\right], \qquad l_1 \leq x \leq l_2 \quad (2)$$

$$\Psi^{(3)} = \sum_{n=0}^{\infty} C_n \sin\left(k_{xn}^{(3)} x\right) \cos\left[\frac{n\pi}{b}(y - b/2)\right], \qquad (l_1 + l_2) \leq x \leq (l_1 + l_2 + w) \quad (3)$$

and

$$\Psi^{(4)} = \sum_{n=0}^{\infty} D_n \cos\left(k_{xn}^{(4)} x\right) \cos\left[\frac{n\pi}{b}(y - b/2)\right], \qquad (l_1 + l_2 + w) \leq x \leq a. \quad (4)$$

For the regions (1), (3), and (4) the separation equation

$$k_{xn}^{(i)2} + \left(\frac{n\pi}{b}\right)^2 + \beta^2 = \epsilon_r^{(i)} k_0^2, \qquad i = 1,3,4 \quad (5)$$

holds, while for the ferrite filled region (2) the separation equation is [10]

$$k_{xn}^{(2)2} + \left(\frac{n\pi}{b}\right)^2 + \beta^2 = \omega^2 \epsilon^{(2)} \mu_{\text{eff}} \quad (6)$$

and

$$k_0^2 = \omega^2 \epsilon_0 \mu_0 = (2\pi f)^2 \epsilon_0 \mu_0. \quad (7)$$

The effective permittivity μ_{eff} of the ferrite is calculated from the permittivity tensor $\vec{\vec{\mu}}$ as

$$\mu_{\text{eff}} = \frac{\mu_1^2 - \mu_2^2}{\mu_1} \quad (8)$$

with

$$\vec{\vec{\mu}} = \mu_0 \begin{pmatrix} \mu_1 & 0 & j\mu_2 \\ 0 & 1 & 0 \\ -j\mu_2 & 0 & \mu_1 \end{pmatrix} \quad (9)$$

$$\mu_1 = 1 + \frac{\omega_M \omega_L}{\omega_L^2 - \omega^2} \quad (10)$$

$$\mu_2 = \frac{\omega \omega_M}{\omega_L^2 - \omega^2}. \quad (11)$$

The quantities ω_M and ω_L are related to the gyromagnetic ratio γ, the saturation magnetization M_s, and the bias magnetic field H_0 as

$$\omega_M = \gamma M_s \quad (12)$$

$$\omega_L = \gamma H_0. \quad (13)$$

The magnetic and electric field components are calculated from the potentials using standard methods. The continuity condition for the fields at the boundaries at $x = l_1$, $x = l_1 + l_2$, and $x = l_1 + l_2 + w$ lead to a system of integral eigenvalue equations, which, using the Ritz-Galerkin method as described in [6], is converted into a system of inhomogeneous equations

$$\vec{F} \cdot \boldsymbol{A} = 0 \quad (14)$$

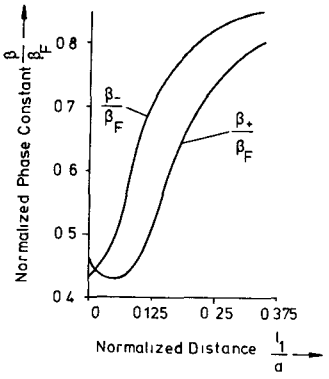

Fig. 3. The phase constants of the foreward and the backward traveling waves normalized to the phase constant $\beta_F = 253$ rad/m of an unloaded fin line (fin line without ferrite slab; Fig. 1), plotted as a function of the distance of the ferrite slab from the waveguide wall. ($a = 22.86$ mm, $b = 10.16$ mm, $2s = 3.0$ mm, $l_1 = 5.0$ mm, $l_2 = 1.28$ mm, $w = 0.6$ mm, $\epsilon_r = 10.5$, $f = 11$ GHz, $4\pi M_s = 1300$ A/cm, and $H_0 = 2780$ A/cm.)

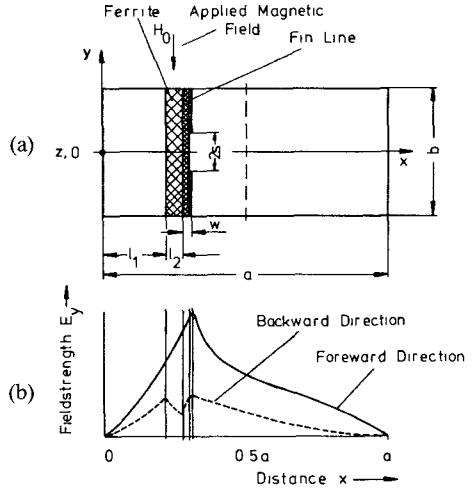

Fig. 4. (a) Cross-sectional structure of a fin-line isolator; (b) with the calculated field distribution for the foreward and the backward direction at $y = 0$.

with $\vec{F}$ as the system matrix and A the amplitude vector. This eigenvalue equation can be solved when a zero of the system determinant is found

$$\det(\vec{F}) = 0 \tag{15}$$

thus yielding the phase constant and the field distributions of the waves propagating on the ferrite loaded fin line. For practical calculations the size of the system was truncated to a number of about 20 equations to achieve satisfactory convergence of the results.

As an example of the results achieved with the calculation method, in Fig. 3 the phase constants of the foreward and the backward traveling waves in the structure are plotted versus the distance of the ferrite slab from the waveguide wall. As can be seen in this example a differential phase shift may be achieved with a maximum value of about 6°/mm for $l_1/a \cong 0.125$.

In Fig. 4 the calculated field distributions for the waves on the ferrite-loaded fin-line structure are shown. It is seen that the effect of the ferrite slab is to displace the fields of the guided modes similar to the field displacement arrangements in metal waveguide isolators.

The two possible ways to exploit the field displacement for an isolator design are: 1) to place an absorbing medium left to the ferrite slab ($x < l_1$) so that more power is dissipated of the foreward traveling wave than is of the backward traveling wave; or 2) to place a thin absorbing sheet (resistive card) at the interface between the ferrite region and the dielectric region $x = l_1 + l_2$, so that more power is dissipated of the backward traveling wave than is of the foreward traveling wave. It has to be noted that for neither case the calculated example presented here would yield an acceptable isolation. Rather, the example is to show that using the calculation method presented, the structure may be analyzed and optimized; to get analytical values for the design of isolators the theory has to be developed further.

IV. Experimental Isolator

Fig. 5 shows a photograph of the fin-line structure designed to prove the feasibility of a field displacement isolator in fin-line technique.

A section of fin line with tapered transitions for insertion into a waveguide measurement setup [8] is layered on its back side with a composition of a dielectric spacer, a ferrite slab and an absorbing sheet. The ferrite, spacer, and absorber are tapered at the ends to enhance the match to the fin line. The cross-sectional view of the loaded fin-line structure is given in Fig. 6 together with the desired field patterns to achieve isolator action as discussed under 1) in Section III. For waves propagating in the transmission direction it is supposed that the electromagnetic fields are shifted away from the ferrite slab, while for waves in the opposite direction it is supposed that the fields are strong near the ferrite slab. Thus the absorber sheet dissipates a large portion of the energy traveling in the isolated direction (shaded area in Fig. 6(b)) while only little energy is absorbed in the transmission direction (shaded area in Fig. 6(c)).

Since so far no theoretical investigation was carried out

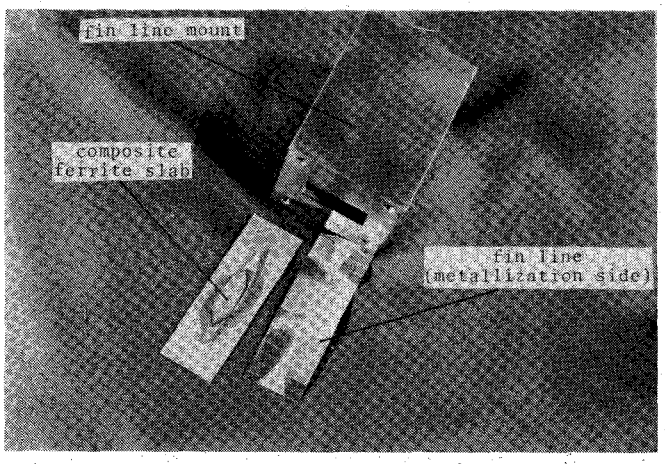

Fig. 5. Photograph of the experimental fin-line isolator.

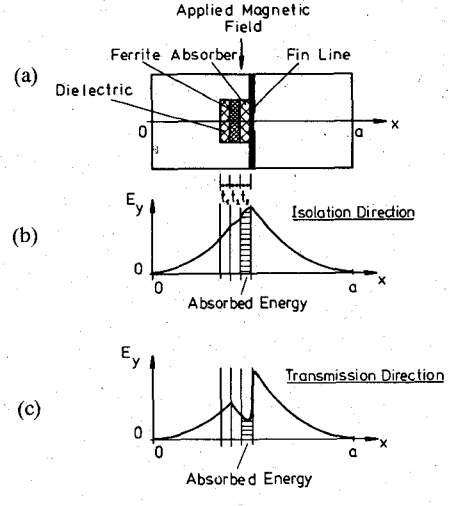

Fig. 6. (a) Cross-sectional structure of the investigated isolator; (b) with the desired field distribution for the isolated direction; and (c) for the transmission direction.

to determine the optimum thickness and dielectric loading of the ferrite slab, the best permittivity of the dielectric spacer, and the optimum position of the absorber, some of these parameters were checked experimentally. So, in a series of experiments, the permittivity and the thickness of the dielectric spacer and the dimensions of the absorber were varied. Best results with a figure of merit (reverse loss to forward loss) around 25 were achieved using a low-permittivity spacer ($\epsilon_r = 2.33$) of a thickness $t_1 = 079$ mm and a ferrite slab ($M_s = 1300$ A/cm) of thickness $t_2 = 1.28$ mm, while the absorber (Ferrosorb epoxy sheet) had a thickness of $t_3 = 1.0$ mm. The length of the composite slab structure was 22 mm, including 11 mm for both tapered ends. The applied magnetic field was 2780 A/cm.

In Fig. 7 the measured isolator characteristics are plotted for this design. The achieved isolation bandwidth still is small, but it was found that this can be increased using a more effective absorber load. On the other hand the minimum transmission loss of 0.9 dB is encouraging since it includes a measured 0.5-dB insertion loss for the unloaded fin-line section.

Very much larger bandwidths have been achieved using

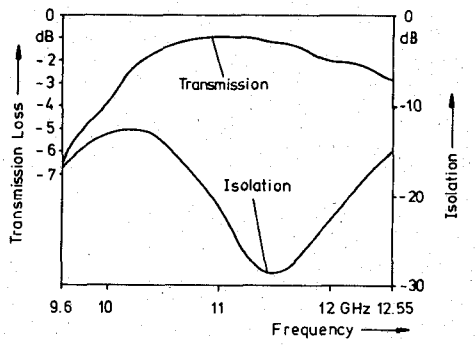

Fig. 7. The measured isolation and transmission loss of the experimental fin-line isolator.

a tighter coupling of the ferrite slab to the fin line ($t_1 = 0$) at the expense of an increased transmission attenuation. This mode of operation also has been employed in a slot-line isolator in the past [9].

V. Conclusions

A field expansion approach for the investigation of the ferrite-loaded fin line has been presented, which can be considered as an extension of the well-known field expansions methods for fin line with an additional ferrite layer.

First theoretical results for the phase constants and the field distributions show the potential of the method to help in the optimization of realistic fin-line isolators. Furthermore it has been shown experimentally that fin-line isolators are feasible. Improvements of the present design are expected from the use of resistive card absorbers and further matching of the ferrite loaded fin line to the unloaded fin line.

Great advantages of the described isolator structure could be that it is easily integratable into fin-line circuits by simply loading a suitable section of fin line with a composite ferrite slab. Furthermore it could be made extremely compact since the magnet needed to supply the static magnetic field could be integrated into the metal waveguide mount without seriously disturbing the propagating waves, since it is possible to concentrate the propagating waves in the neighborhood of the slot (low-impedance fin lines).

This contribution is intended to trigger further work, particularly field-theoretical investigations of the ferrite loaded fin line. This could yield data needed for a more rigorous optimization of the many parameters in the fin line and the composite ferrite slab.

References

[1] P. J. Meier, "Integrated fin-line millimeter components," *IEEE Trans. Microwave Theory Tech.*, vol. MTT-22, 1209–1216, 1974.
[2] H. Hofmann, H. Meinel, and B. Adelseck, "New integrated mm-wave components using fin-lines," in *IEEE MTT-S Symp. Dig.*, 1978, pp. 21–23.
[3] R. Knöchel, "Design and performance of microwave oscillators in integrated fin-line technique," *Int. J. Microwaves, Optics Acoustics (MOA)*, vol. 3, pp. 115–120, 1979.
[4] H. Hofmann, "Dispersion of planar waveguides for millimeter-wave application," *Arch. Elek. Uebertragung.*, vol. 31, pp. 40–44, 1977.
[5] W. J. Hoefer, "Fin-line design made easy," in *IEEE MTT-S Symp. Dig.*, pp. 471–473.

[6] A. Beyer and I. Wolff, "The solution of the earthed fin line with finite metallization thickness," in *IEEE MTT-S Symp. Dig.*, 1980, pp. 258–260.
[7] P. J. B. Clarricoats, *Microwave Ferrites*. London: Chapman & Hall, 1961.
[8] A. Beyer and I. Wolff, "Calculation of the transmission properties of inhomogeneous fin lines," in *Proc. 10th European Microwave Conf., 1980*, pp. 322–326.
[9] L. Courtois and M. De Vecchis, "A new class of nonreciprocal components using slot line," *IEEE Trans. Microwave Theory Tech.*, vol. MTT-23, pp. 511–516, June 1975.
[10] A. G. Gurevich, *Ferrites at Microwave Frequencies*. New York: Consultants Bureau, 1963.

Adalbert Beyer, photograph and biography not available at the time of publication.

Klaus Solbach (M'80), for a photograph and biography please see page 77 of the January issue of this TRANSACTIONS.

Integrated Circuit Compatible Surface Acoustic Wave Devices on Gallium Arsenide

THOMAS W. GRUDKOWSKI, MEMBER, IEEE, GARY K. MONTRESS, MEMBER, IEEE, MEYER GILDEN, MEMBER, IEEE, AND JAMES F. BLACK, MEMBER, IEEE

Abstract—**Improvements in gallium arsenide materials technology have led to the rapid development of GaAs MIC [1], CCD [2], and digital IC [3] technologies in the last several years. In this paper we consider the additional capabilities afforded by the inherent piezoelectric properties of GaAs [4]. The primary emphasis of the work is on surface acoustic wave (SAW) device configurations using MESFET and Schottky-barrier diode fabrication techniques which are compatible with the eventual monolithic integration of electronic devices on the same substrate. The GaAs SAW technology described here provides a means for achieving electronically variable delay, high-Q resonator structures for VHF/UHF oscillator frequency control, and real-time signal processing operations such as convolution and correlation. Prototype device designs and performance are described, including two-port GaAs SAW resonators with Q's as large as 13 000 at 118 MHz and a programmable GaAs SAW PSK correlator capable of signal correlation at 10-MHz chip rates. Further GaAs SAW device development required for increasing the operating frequency range to 500 MHz and processing bandwidth to 100 MHz is indicated.**

I. INTRODUCTION

THE CAPABILITIES of GaAs technology for meeting the advanced requirements of analog and digital system designs are increasingly evident. These capabilities are based for the most part on the superior semiconducting properties of GaAs as compared to silicon. In particular, the larger electron mobility and wider bandgap of GaAs provide the means for achieving higher device operating frequency, speed, and temperature. In addition, the availability of semi-insulating GaAs substrate material makes the extension of device operating frequency into the microwave region possible and allows for great flexibility in the techniques used for device interconnection.

In this paper we describe some of the fundamental aspects of SAW device operation on GaAs as well as several new and promising device developments. By using an n-type semiconducting layer on a semi-insulating GaAs substrate one may combine the piezoelectric and semiconducting properties either indirectly or directly. For example, these properties may be treated separately by fabricating SAW delay lines, resonators, or filters on the semi-insulating substrate and combining these components with electronic components fabricated on an adjacent epitaxial or ion-implanted semiconducting layer using thin film interconnects. Alternatively, the SAW/electronics coupling may be performed directly through acoustoelectric interaction of the SAW electric field with the charge carriers or the potential distribution within a diode or FET. Either approach leads to monolithic device designs which may reduce circuit size, power consumption, and cost as compared to hybrid approaches and also extends the capabilities and design options available for GaAs IC development.

The SAW device configurations described here typically operate within the 100–200-MHz frequency range although extension to 1 GHz is feasible, limited primarily by increasing propagation loss [5]. The use of a nominal ⟨001⟩ oriented substrate is consistent with that used for GaAs IC

Manuscript received April 13, 1981; revised August 5, 1981. This work was supported in part by USAERADCOM under Contract DAAK20-79-C-0263 and by the Rome Air Development Center under Contract F19628-79-C-0056.

The authors are with United Technologies Research Center, East Hartford, CT 06108.

0018-9480/81/1200-1348$00.75 ©1981 IEEE